Supplementary information

Single-cell metabolic profiling of human cytotoxic T cells

In the format provided by the
authors and unedited

Supplementary Material for: Single-cell metabolic profiling of human cytotoxic T cells

Felix J. Hartmann[1], Dunja Mrdjen[1], Erin McCaffrey[1,2], David R. Glass[1,2], Noah F. Greenwald[1], Anusha Bharadwaj[1], Zumana Khair[1], Sanne G.S. Verberk[3], Alex Baranski[1], Reema Baskar[1], William Graf[4], David Van Valen[4], Jan Van den Bossche[3], Michael Angelo[1], Sean C. Bendall[1*]

Affiliations:

[1]Department of Pathology, School of Medicine, Stanford University, Palo Alto, California, USA

[2]Immunology Graduate Program, Stanford University, Palo Alto, California, USA

[3]Department of Molecular Cell Biology and Immunology, Amsterdam Cardiovascular Sciences, Cancer Center Amsterdam, Amsterdam UMC, Vrije Universiteit Amsterdam, Amsterdam, Netherlands

[4]Division of Biology and Biological Engineering, California Institute of Technology, Pasadena, California, USA

[*]Correspondence: bendall@stanford.edu

Supplementary Figures

Supplementary Figure 1: Assay-specific validation of heavy-metal conjugated metabolic antibodies.

Supplementary Figure 2: Robustness and reproducibility of the scMEP approach.

Supplementary Figure 3: Metabolic protein expression is not explained by cell volume and mitochondrial mass.

Supplementary Figure 4: Metabolic profiles recapitulate dynamic changes in metabolic pathway activity.

Supplementary Figure 5: Single-cell metabolic regulome profiles of inflammatory macrophage activation.

Supplementary Figure 6: Coordination of metabolic remodeling in human T cells.

Supplementary Figure 7: Low dose oligomycin influences metabolic remodeling and proliferation of human CD8$^+$ T cells.

Supplementary Figure 8: scMEP recapitulates metabolic differences of human naïve and memory T cells.

Supplementary Figure 9: Identification of metabolic phenotypes of immune cell lineages across human tissues.

Supplementary Figure 10: Metabolic and immunological subsets of human CD4$^+$ T cells across tissues.

Supplementary Figure 11: Immunohistochemistry validation of metabolic antibodies.

Supplementary Figure 12: Imaging-based analysis of metabolic states in human colorectal carcinoma.

Supplementary Figure 13: Imaging-based analysis of metabolic CD8$^+$ T cell subsets.

a Mass cytometry-based validation of heavy metal-conjugated antibodies

Cell lines — 293T (0.0), A549 (4.9), ES-H9 (4.7), HCT-116 (1.8), HEL (4.7), HELA (4.5), Jurkat (2.5), NCIH460 (4.4), NTERA (0.0), Ramos (3.3), REH (2.9), THP-1 (3.9), U937 (2.7)

GLUT1-167Er (EPR3915)
Positivity treshold: PASS
Differential expression: PASS

Whole blood — T cells CD4 (0.7), T cells CD8 (1.0), B cells (2.5), NK cells (1.7), Monocytes (0.4), cDCs (0.0), pDCs (4.4), Basophils (0.1), Neutrophils (0.0)

GLUT1-167Er (EPR3915)
Positivity treshold: PASS
Differential expression: PASS

T cell activation — resting (0.2), aCD3/aCD28 (4.7)

GLUT1-167Er (EPR3915)
Positivity treshold: PASS

Cell lines — 293T (0.2), A549 (0.3), ES-H9 (0.5), HCT-116 (0.0), HEL (0.4), HELA (0.6), Jurkat (0.2), NCIH460 (0.0), NTERA (0.7), Ramos (0.1), REH (0.1), THP-1 (0.2), U937 (0.0)

ATGL-166Er (AT2G2)
Positivity treshold: FAIL
Differential expression: NA

Whole blood — T cells CD4 (0.0), T cells CD8 (0.0), B cells (0.0), NK cells (0.0), Monocytes (0.1), cDCs (0.1), pDCs (0.1), Basophils (0.1), Neutrophils (0.1)

SOD2-143Nd (MnS-1)
Positivity treshold: FAIL
Differential expression: NA

T cell activation — resting (0.5), aCD3/aCD28 (0.6)

MCT1-150Nd (882616)
Positivity treshold: FAIL

b Tissue-based validation of heavy metal-conjugated antibodies
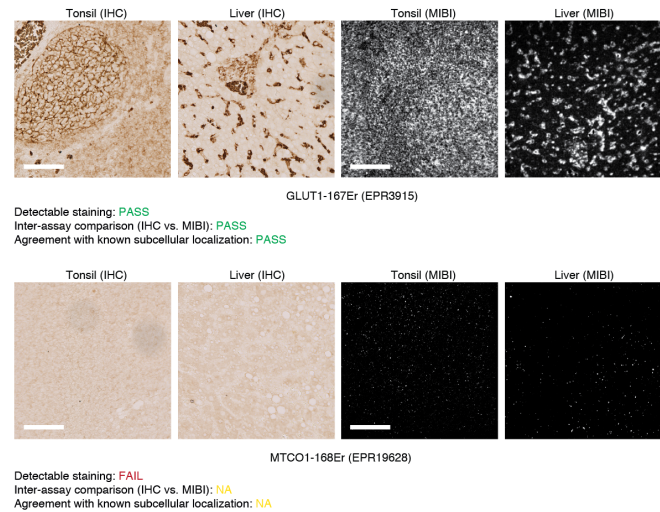
Tonsil (IHC) — Liver (IHC) — Tonsil (MIBI) — Liver (MIBI)

GLUT1-167Er (EPR3915)
Detectable staining: PASS
Inter-assay comparison (IHC vs. MIBI): PASS
Agreement with known subcellular localization: PASS

Tonsil (IHC) — Liver (IHC) — Tonsil (MIBI) — Liver (MIBI)

MTCO1-168Er (EPR19628)
Detectable staining: FAIL
Inter-assay comparison (IHC vs. MIBI): NA
Agreement with known subcellular localization: NA

Supplementary Figure 1: Assay-specific validation of heavy-metal conjugated metabolic antibodies. a, A broad range of cell lines was stained with heavy-metal conjugated antibodies and analyzed by mass cytometry (left). Human peripheral blood stained with lineage markers (CD45, CD3, CD4, CD8, CD45RA, CD66, CD14, CD19, CD20, HLA-DR, CD56, CD57, CD11c, CD123, FceRI, CD235ab) and metabolic antibodies to be validated (middle). Major immune cell types were identified using cell lineage markers and manual gating. Human T cells (resting and activated with anti-CD3/anti-CD38-beads for 72 h) stained with metabolic antibodies (right). Numbers in brackets represent median arsinh values for the indicated population. Positive staining was defined as median >10 ion counts, equal to asinh transformed value >1.5 of any subpopulation. Example of an antibody passing indicated quality control metrics (top) and range of examples of antibodies failing indicated metrics at various stages (bottom). Where available, cell-lineage specific expression and induction upon activation were compared to previously determined values (Uhlen et al., 2015). **b**, Staining of control tonsil and liver FFPE tissues with metabolic antibodies analyzed through traditional IHC (left) and MIBI-TOF (right). Detectable staining was determined through visual inspection of both IHC and grayscale MIBI-TOF images. For intra-assay quality control, IHC and MIBI-TOF images were visually compared and in addition, related to previously determined staining patterns (Uhlen et al., 2015). Shown are examples of an antibody passing (top) or failing (bottom) the indicated quality control metrics. Scale bars = 100 μm. All validations were performed once for each assay and repeated at least once more in case of negative or unclear results. Final outcomes of this validation procedure for all antibodies are summarized in Supplementary Table 2.
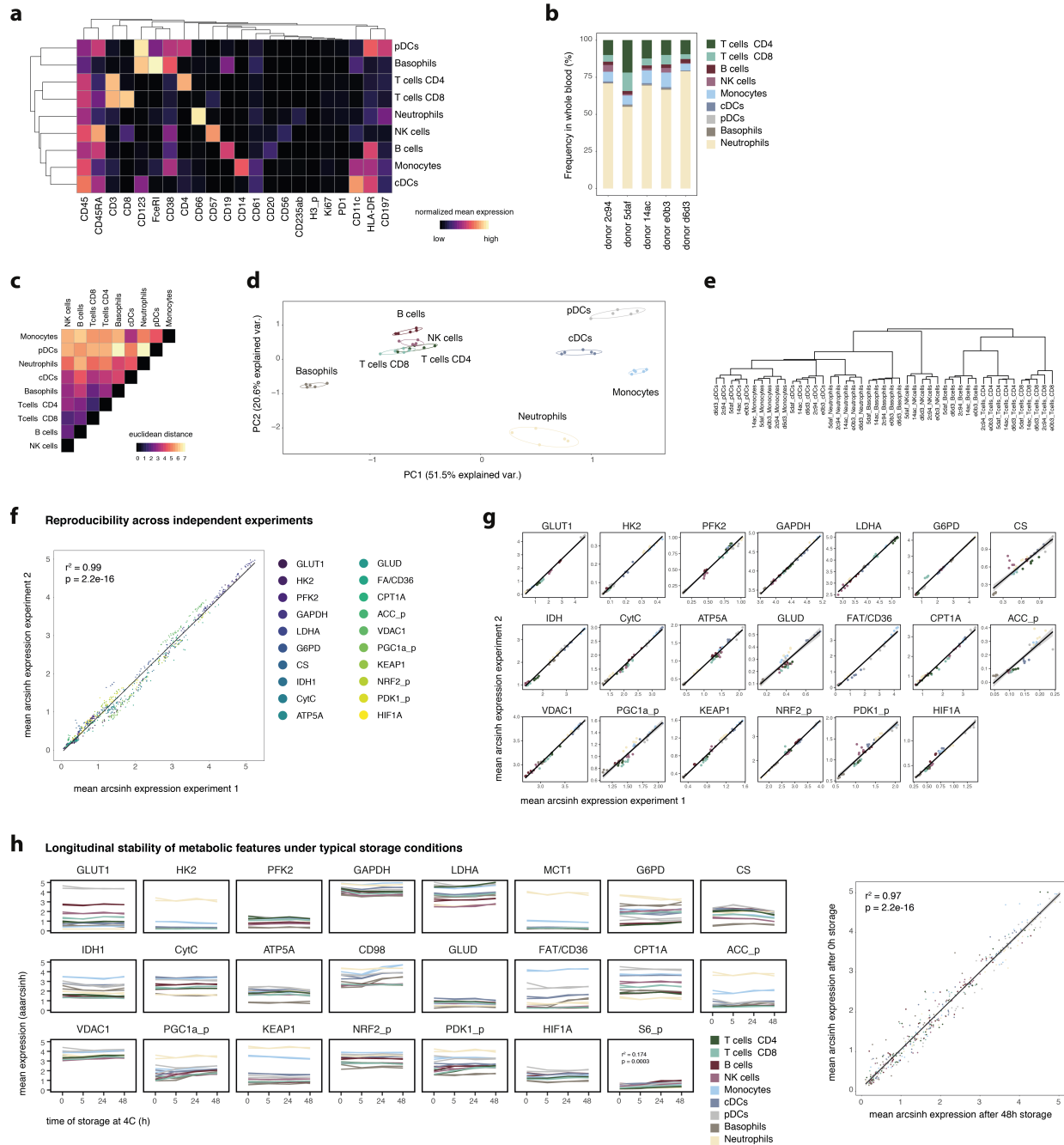
Supplementary Figure 2: Robustness and reproducibility of the scMEP approach. Whole blood of healthy individuals (N = 5, see Supplementary Table 2) was fixed and stained with 23 metabolic and 22 immunological probes. **a**, Cell populations were identified through FlowSOM clustering (CD45, CD3, CD4, CD8, CD45RA, CD66, CD14, CD19, CD20, HLA-DR, CD56, CD57, CD11c, CD123, FceRI, CD235ab) and annotated into the major immune cell lineages. Shown here are mean normalized (99.9th percentile) expression values (asinh transformed) across identified peripheral immune cell populations. **b**, Frequencies of immune cells as identified in a across the five healthy donors. **c**, Euclidean distances between immune cell lineages based on the high-dimensional metabolic space (23 features). **d**, First two components of a principal component analysis (PCA) of immune cell lineages as defined before, using only metabolic profiles and no immune markers. Each point represents one immune cell population from one healthy donor. Axes are scaled to the percentage of variance explained by the respective principal component. **e**, Hierarchical clustering (only using metabolic targets) of immune cell lineages from the five healthy individuals. **f**, Cells from the five healthy individuals as in a were stained and analyzed in two independent experiments using a highly similar panel and immune

cell lineages were assigned as in a. Each point represents a mean asinh transformed value of one metabolic marker in one immune cell lineage. Points are colored by the respective metabolic probe. The black line as well as the r^2 and P-value (P = 2.2e-16) show the results of a linear regression model. **g**, Mean arsinh values as in f for each marker separately. Colors indicate the respective immune cell population. **h**, Whole blood (two technical replicates) was drawn into a sodium heparin tube and either processed (red blood cell lysis and fixation) immediately or stored at 4 °C for up to 48 h before processing. All samples were then barcoded into a composite sample and analyzed as before. Charts show mean asinh-transformed values for each metabolic marker on a given immune cell lineage across time (left). Linear regression between mean population values of the 0 and 48 h storage times. The black line, the r^2 and the P-value (P = 2.2e-16) show the results of a linear regression model.
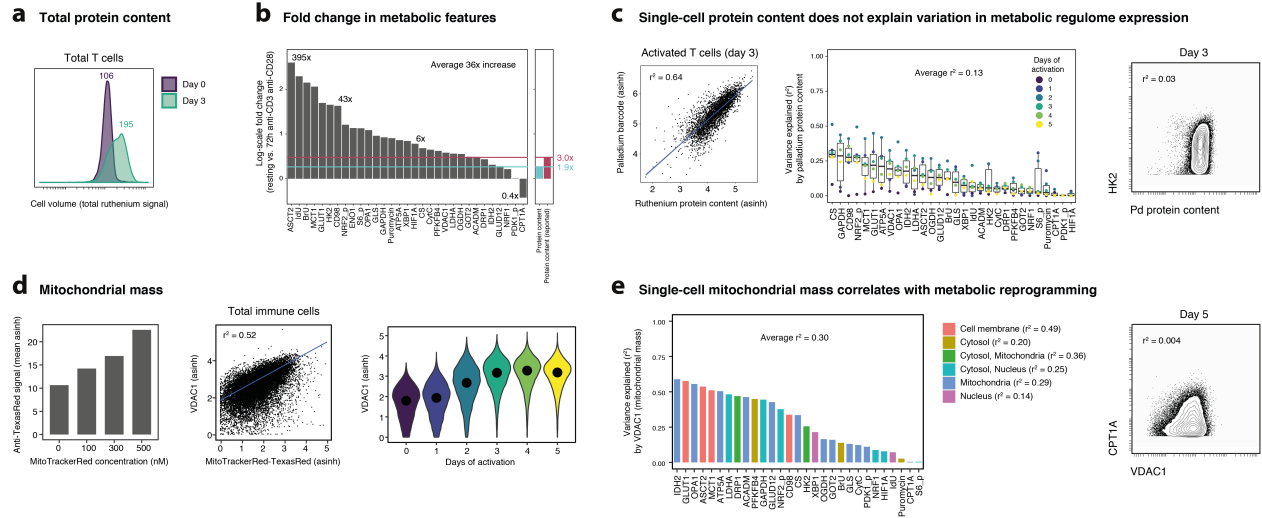
Supplementary Figure 3: Metabolic protein expression is not explained by cell volume and mitochondrial mass. a, Human T cells were activated with anti-CD3, anti-CD28 beads for 0 and 3 days and total protein content was determined by mass cytometry using an amine-reactive ruthenium compound. **b**, Fold changes in metabolic regulator expression were calculated as asinh-differences between resting and 72 h-activated human naïve CD8^{+} T cells. Changes in protein content were determined as in a (blue) or taken from the literature (red) (Geiger et al., 2016; Howden et al., 2019). **c**, Human T cells activated for 72 h were stained with amine-reactive palladium compounds used for cellular barcoding and ruthenium compounds as in a (left). Blue line and r^2 values represent results of a linear regression model, with black shading representing the 95% CI. r^2 values between palladium protein signal and metabolic marker expression for 0-5 days of T cell activation (middle). Lines indicate median values, boxes indicate interquartile range (IQR), hinges extent to ±1.5 IQR. Example of minimal correlation between a metabolic feature (HK2) and total protein content (right). **d**, Human T cells were incubated with the indicated concentrations of Mitotracker Deep Red, fixed, MeOH-permeabilized and stained with a heavy metal-conjugated anti-TexasRed fluorophore antibody (left). Blue line and r^2 values represent results of a linear regression model, with black shading representing the 95% CI (middle). VDAC1 signal across days of activation (right). Black circles indicate population medians (right). **e**, r^2 values of single-cell linear regression between VDAC1 and the indicated metabolic regulators. Cell compartments were identified through the uniprot database and the human cell atlas (left). Example of minimal correlation between two mitochondrial markers (right).
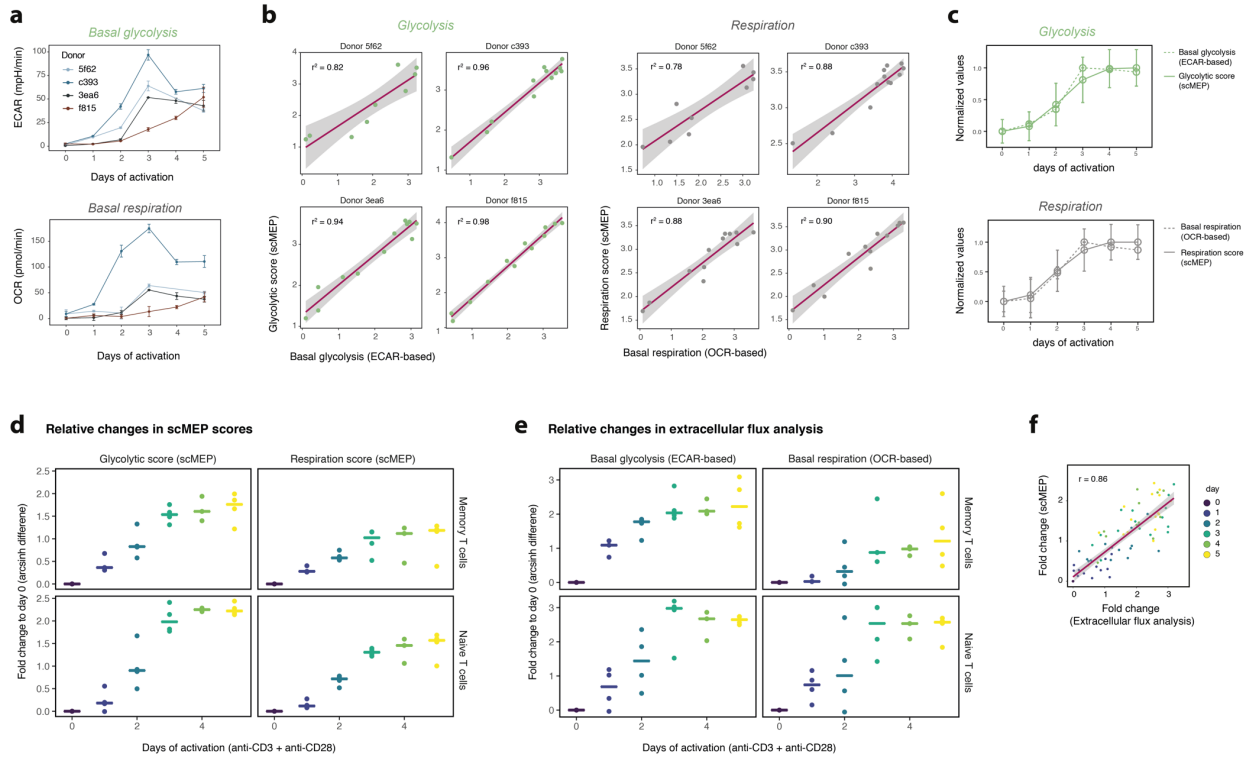
Supplementary Figure 4: Metabolic profiles recapitulate dynamic changes in metabolic pathway activity. a, PBMCs were isolated from healthy donors (N = 4). Naïve or memory T cells (containing CD4^{+} and CD8^{+} cells) were purified by negative isolation with magnetic beads. Purified T cell populations (naïve or memory) were then activated using anti-CD3/anti-CD28 beads for 0-5 days. Shown are extracellular flux analysis-derived basal glycolysis (ECAR-based, top) and basal respiration (OCR-based, bottom) across different days of activation and across multiple independent donors. Circles and error bars represent mean±s.d. between technical replicates (wells) for each donor. **b,** Circles represent the mean (of all single cells) scMEP score of a T cell population (naïve or memory) stimulated with anti-CD3/anti-CD28 for 0-5 days. Red lines and r^2 values represent results of a linear regression model, with black shading representing the 95% CI. **c,** Normalized (minimum to maximum scaled) glycolytic (top) and respiration (bottom) scores across days of stimulation. Shown is data for one individual (out of N = 4 independent experiments). Circles represent normalized means. Error bars represent ±s.d. for technical replicates (three replicate measurements from different wells in extracellular flux analysis and single cell values for scMEP scores). **d,** Mass cytometry-based scMEP scores (glycolysis left, respiration right) as in b. Circles represent the mean scMEP score of a T cell population of one donor (memory top, naïve bottom). Fold changes were calculated as difference in asinh values between day 0 and the respective day. Lines represent median values across independent experiments. **e,** Extracellular flux analysis-derived basal glycolysis (ECAR-based, left) and basal respiration (OCR-based, right) across different days of activation and across multiple independent donors. Values were asinh transformed (cofactor 5) and fold changes were calculated as in d. Lines represent median values across the four experiments. **f,** The red line and the r value show the results of a linear regression model with black shading representing the 95% CI.
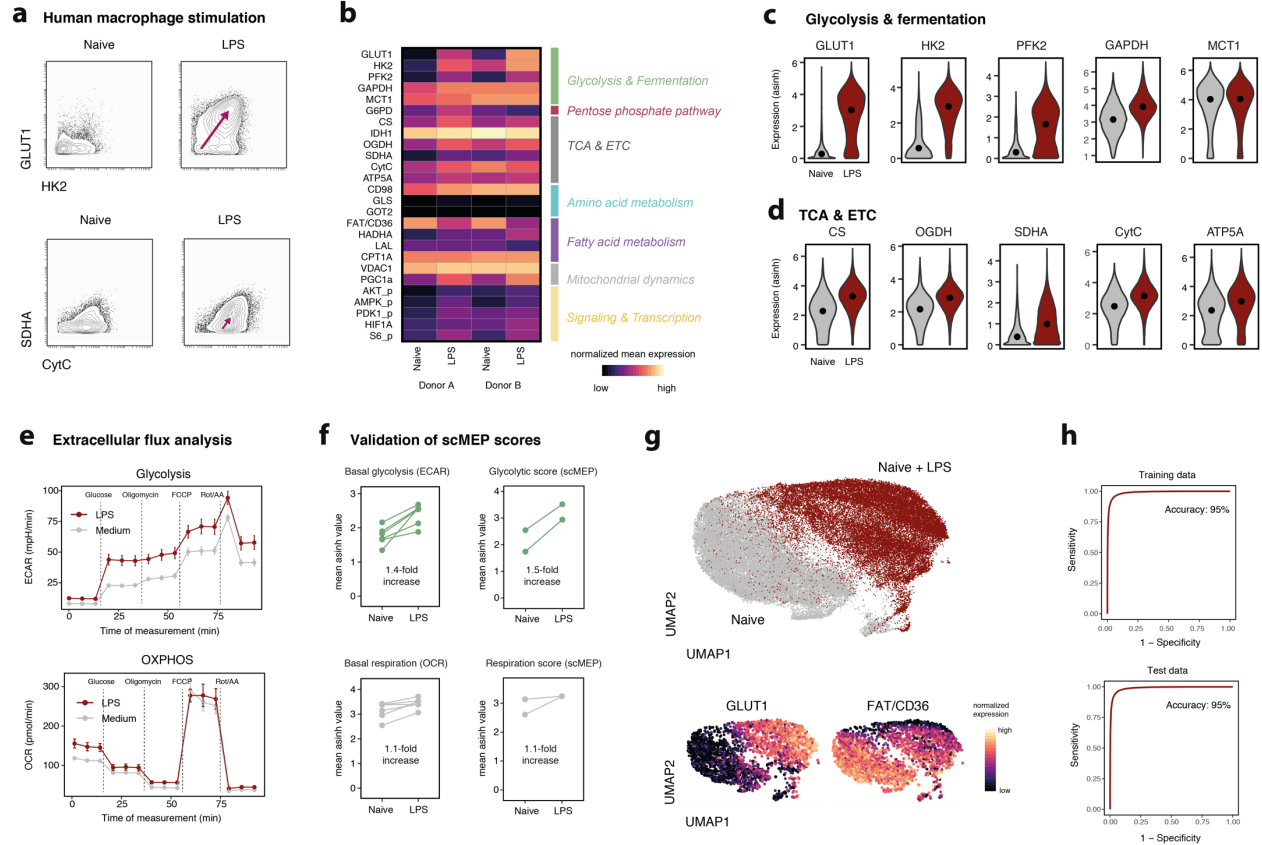
Supplementary Figure 5: Single-cell metabolic regulome profiles of inflammatory macrophage activation. Human peripheral blood monocytes were differentiated into macrophages in the presence of 25 ng/ml M-CSF for 6 days and subsequently cultured for 24 h with or without 10 ng/ml LPS. **a**, Exemplary plots of upregulation of glycolytic (top) and respiratory (bottom) metabolic regulators determined by mass cytometry. **b**, Normalized (99.9th percentile) mean expression of all assessed metabolic regulators in naïve and LPS activated human macrophages from two healthy human donors. **c**, Expression levels of important glycolytic enzymes in naïve (grey) and LPS activated (red) macrophages. Black circles represent population medians. **d**, Expression levels of important TCA/ETC components as in c. **e**, Extracellular flux analysis of human macrophages stimulated using the same protocol as in a-c. Extracellular acidification rate (ECAR; top) and oxygen consumption rate (OCR; bottom) for each measurement following injections of glucose and mitochondrial modifiers to determine basal pathway activity. FCCP = fluoro-carbonyl cynade phenylhydrazon, Rot = Rotenone, AA = antimycin A. Shown is data from one individual (out of N = 4 independent experiments). Circles and error bars represent mean±s.d. for the three technical replicates (wells). **f**, Mean asinh-transformed values of macrophages from 6 human donors analyzed by extracellular flux analysis as in e (left) and two independent donors analyzed by mass cytometry (right). Basal glycolysis = mean($ECAR_{glucose}$) – mean($ECAR_{baseline}$). Basal respiration = mean($OCR_{baseline}$) – mean($OCR_{Rot/AA}$). Protein-based scMEP scores (right) represent the mean expression of all metabolic regulators within a given pathway. Fold changes for Seahorse-based (left) and scMEP-based (right) values were calculated as difference of asinh transformed values **g**, Cells were subsampled for equal representation of both modes of activation. Metabolic features were used as input to UMAP dimensionality reduction and visualization. Cells are colored by their mode of activation (top) and by two exemplary metabolic markers (bottom). **h**, L1 regularized linear regression (using only metabolic regulators) was trained on a subset of cells (training data, top) and tested on a separate set of cells (test data, bottom). Stated numbers report balanced accuracy for the indicated activation.
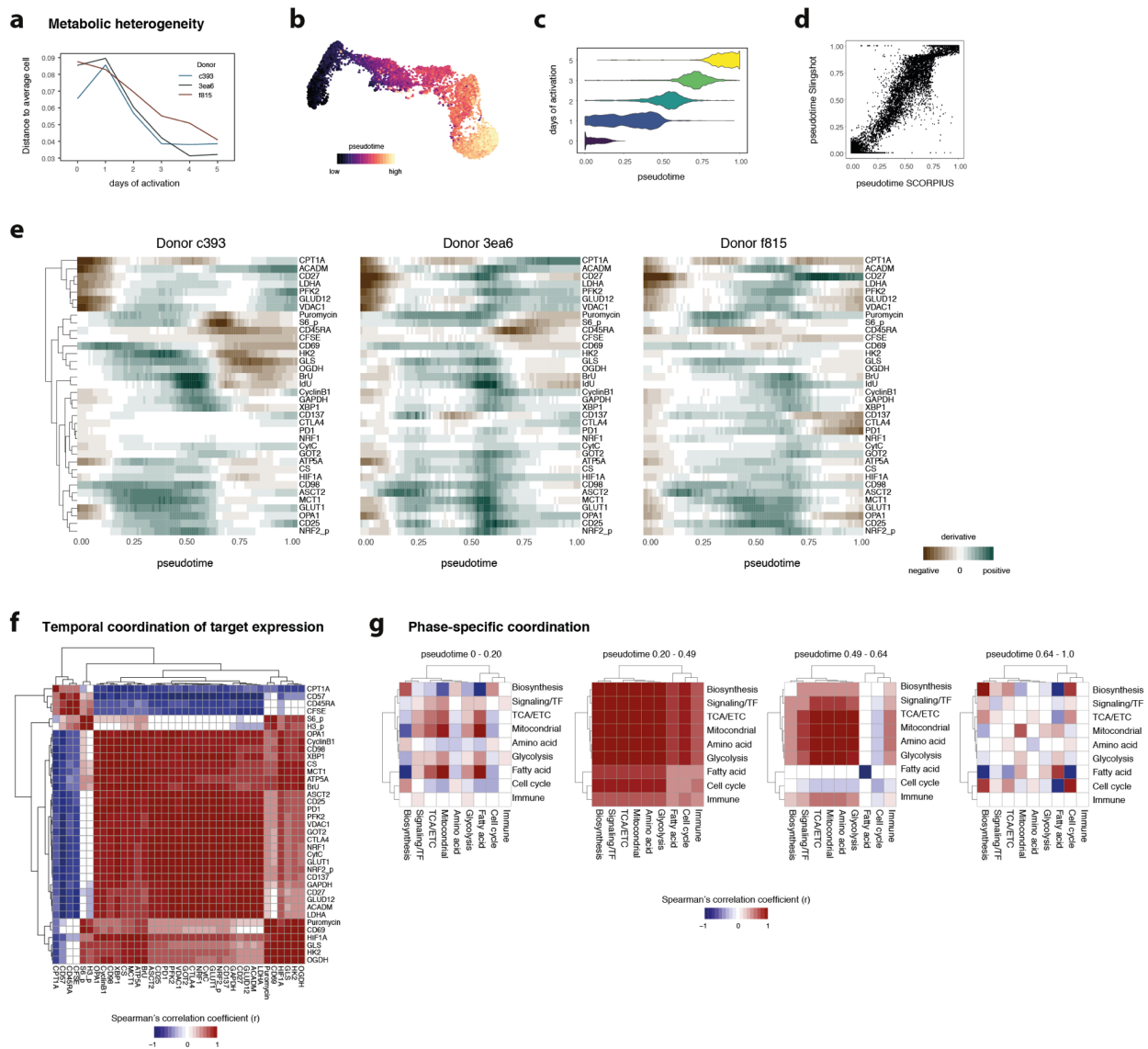
Supplementary Figure 6: Coordination of metabolic remodeling in human T cells. PBMCs were isolated from healthy individuals (N = 3). Naïve T cells (containing $CD4^+$ and $CD8^+$ cells) were purified by negative isolation with magnetic beads. Purified T cell populations were then activated using anti-CD3/anti-CD28 beads for 0-5 days. **a**, Mean metabolic heterogeneity within naïve human $CD8^+$ T cells was calculated as cosine distance (based on all metabolic markers except IdU, but no immune phenotyping markers) to an average cell within the given day of activation. **b**, Cells on a two-dimensional UMAP projection of the high-dimensional space were colored according to their SCORPIUS-inferred pseudotime. **c**, Distribution of cells from different days of activation across pseudotime. **d**, The same cells and the same markers were used to infer pseudotime using an independent algorithm (Slingshot). **e**, Data was binned into 100 bins and averaged for each bin. Slope (first derivative) of marker expression across pseudotime for three independent donors analyzed in three independent experiments. **f**, Binned data as in e was used as an input for Spearman's correlation analysis. P-values were BH-adjusted to correct for multiple hypothesis testing and r values were set to 0 for all BH-corrected P values > 0.05. **g**, Spearman's r as in f stratified by pseudotime bins based on the previously identified inflection points.
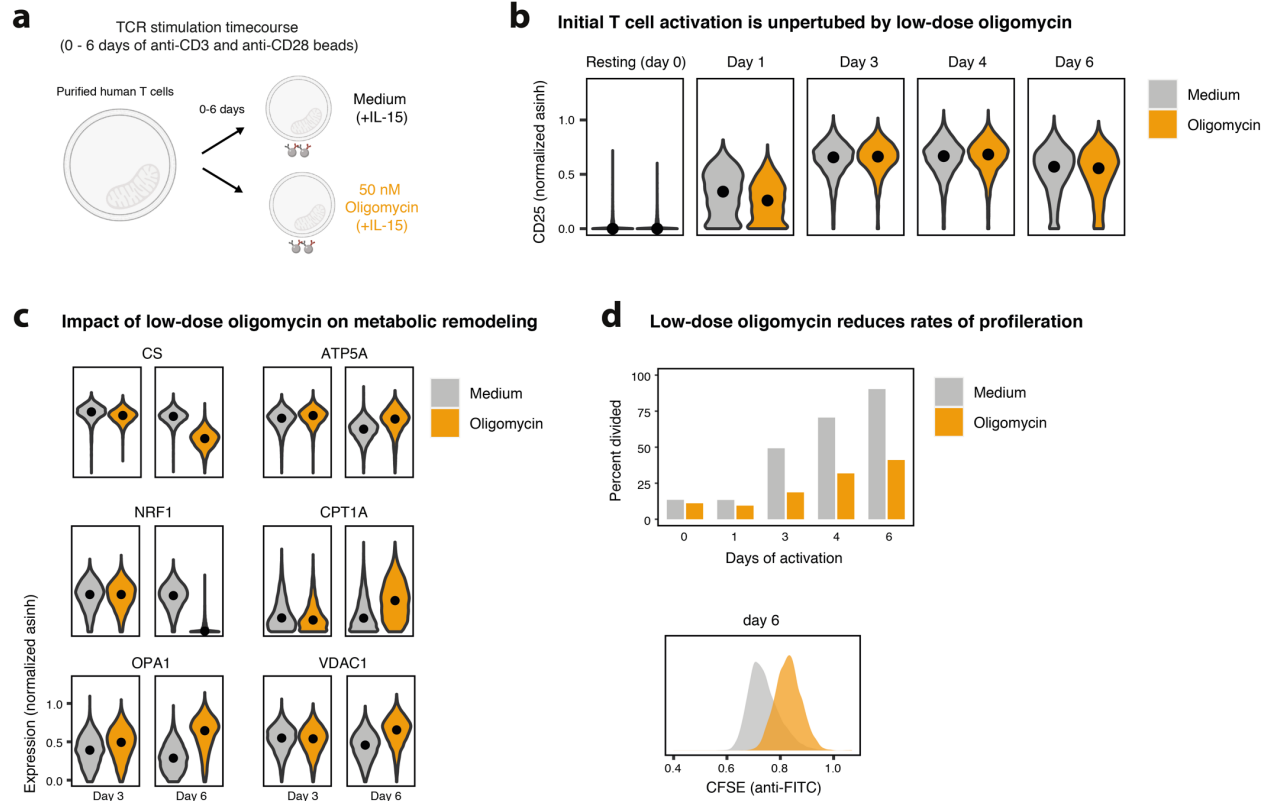
9

Supplementary Figure 7: Low dose oligomycin influences metabolic remodeling and proliferation of human CD8$^+$ T cells.
a, PBMCs were isolated from a healthy individual and memory T cells (containing CD4$^+$ and CD8$^+$ cells) were purified by negative isolation with magnetic beads. Cells were divided into two conditions (medium or 50 nM oligomycin, both supplemented with IL-15) and activated using anti-CD3/anti-CD28 beads for 0-6 days. **b**, Mass cytometry-quantified expression levels of CD25 across different days of CD8$^+$ T cell activation. **c**, Modulation of metabolic protein expression through low dose oligomycin on day 3 (left) and day 6 (right) of anti-CD3/anti-CD28 activation. **d**, Percent divided were gated manually by gating on CFSE signal determined using an anti-FITC antibody (top). Example of raw CFSE signal on day 6 of T cell activation.
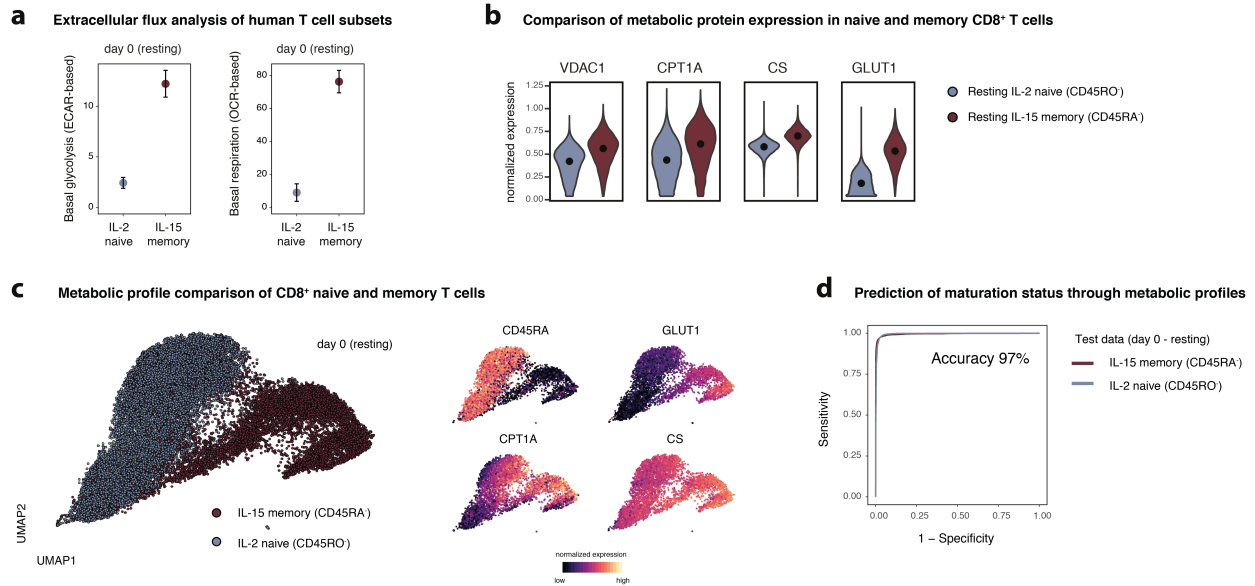
a Extracellular flux analysis of human T cell subsets

b Comparison of metabolic protein expression in naive and memory CD8+ T cells

c Metabolic profile comparison of CD8+ naive and memory T cells

d Prediction of maturation status through metabolic profiles

Supplementary Figure 8: scMEP recapitulates metabolic differences of human naïve and memory T cells. PBMCs were isolated from healthy individuals (N = 3 independent experiments). Naïve T cells (containing CD4+ and CD8+ cells) were purified by negative isolation with magnetic beads. Purified T cell populations were then activated using anti-CD3/anti-CD28 beads for 0-5 days. **a**, Extracellular flux analysis of resting (day 0) IL-2 naïve (CD45RO-) and IL-15 memory (CD45RA-) T cells (containing CD4+ and CD8+). ECAR-based basal glycolysis (left) and OCR-based basal respiration (right). Circles and error bars represent mean±s.d. of the three technical replicates (wells) of one representative donor (out of N = 3 independent experiments). **b**, Examples (one representative donor) of metabolic differences between naïve and memory CD8+ T cells as in a. **c**, Cells were subsampled for equal representation of naïve and memory CD8+ T cells. Two-dimensional UMAP projection of the metabolic space with cells colored by their maturation status (left) or colored by their normalized expression level of markers as in g (right). **d**, L1 regularized linear regression (using only metabolic profiles) was trained on a subset of cells (resting, 0 days of activation) from one donor and tested on a separate set of cells from the same donor. Shown are results from the test dataset and the overall accuracy of the model.
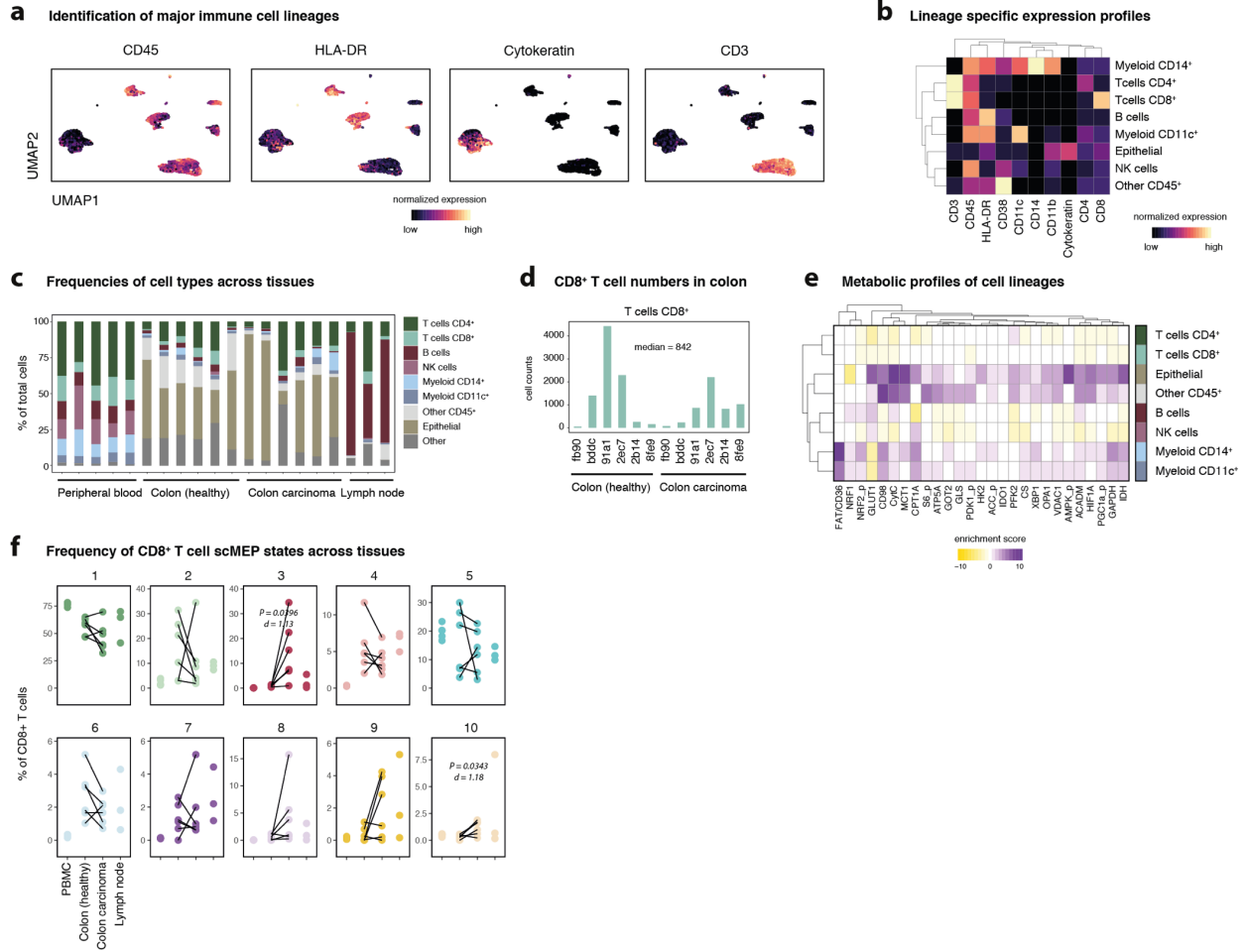
Supplementary Figure 9: Identification of metabolic phenotypes of immune cell lineages across human tissues. Healthy donor PBMC (N = 5), lymph node biopsies (N = 3) as well as single-cell suspensions from colorectal carcinoma (N = 6) and matched adjacent healthy sections (N = 6, see Supplementary Table 2) were barcoded, stained and acquired on a mass cytometer. **a**, Major cell lineages from all samples and tissues were identified through FlowSOM-based clustering. UMAP-dimensionality reduction was calculated using subsampled data from all lineages and all available markers. Cells are colored by their normalized expression value of the indicated lineage markers. **b**, Mean normalized expression values of the major lineage markers across cell populations. **c**, Frequencies of cell populations across all samples. **d**, Total counts of CD8$^+$ T cells from colon samples. **e**, Marker enrichment modeling (MEM) of metabolic features across the major cell lineages. **f**, Statistical analysis of frequencies of scMEP phenotypes within CD8$^+$ T cells. P-values were calculated using a two-sided, paired t-test between healthy and malignant colon sections from the same patient. Welch correction was applied to account for potentially differing variances. Effect size is represented as Cohen's d. scMEP3: Estimate = -13.8, t-statistic = -2.76, CI -26.7 to -0.97, 5 degrees of freedom, BH FDR = 0.198. scMEP10: Estimate = -0.84, t-statistic = -2.89, CI -1.58 to -0.09, 5 degrees of freedom, BH FDR = 0.198. P-values not stated when P > 0.05.
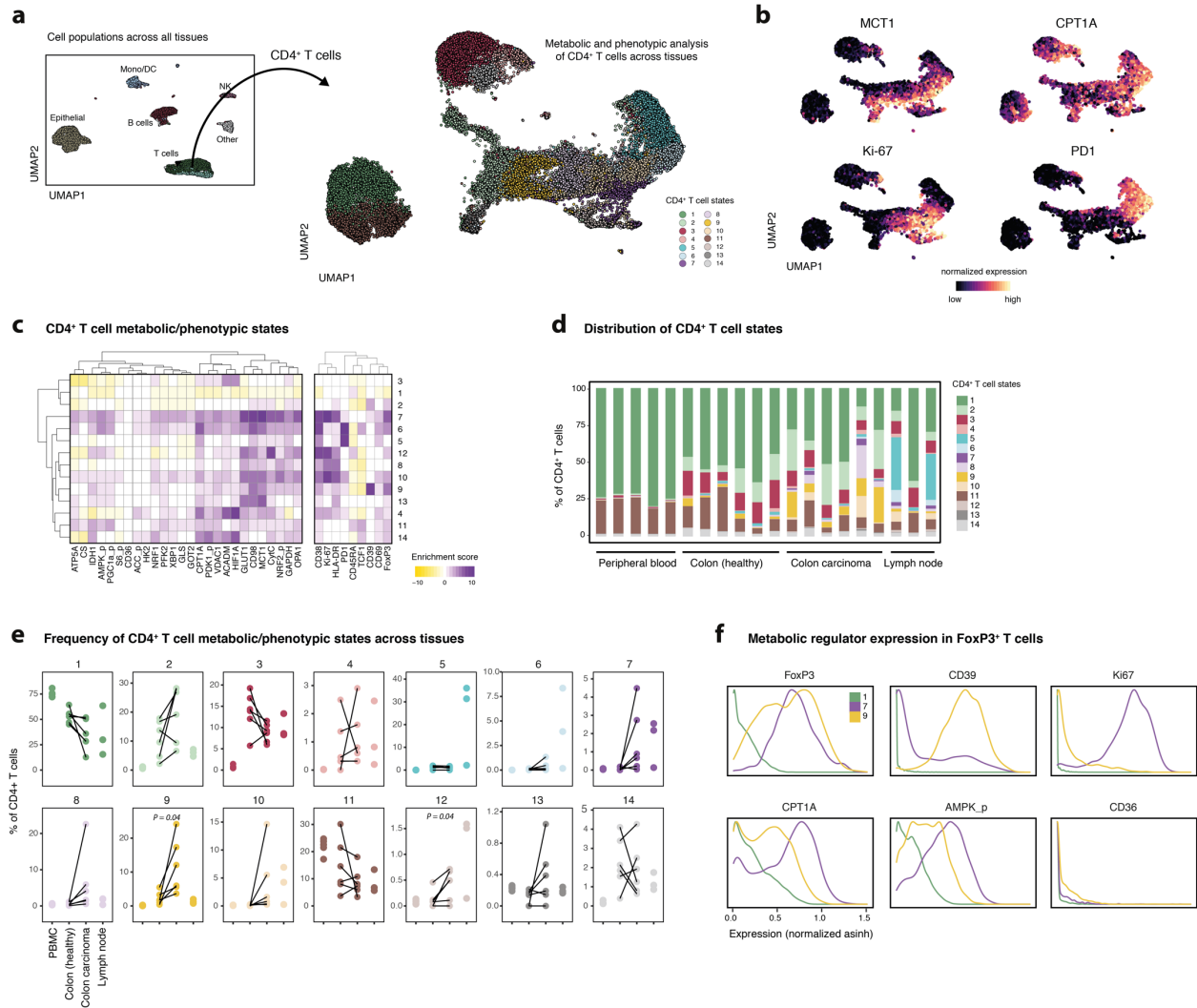
Supplementary Figure 10: Metabolic and immunological subsets of human CD4$^+$ T cells across tissues. Healthy donor PBMC (N = 5), lymph node biopsies (N = 3) as well as single-cell suspensions from colorectal carcinoma (N = 6) and matched adjacent healthy sections (N = 6, see Supplementary Table 2) were barcoded, stained and acquired on a mass cytometer. **a**, Major cell lineages from all samples and tissues were identified through FlowSOM-based clustering. UMAP-dimensionality reduction was calculated using subsampled data from all lineages and all available features (left). Cells are colored by their FlowSOM-based lineage definition. Next, total CD4$^+$ T cells from all samples were selected and metabolic regulators were used to define 14 CD4$^+$ scMEP states, based on FlowSOM clustering. UMAP-dimensionality reduction was calculated using subsampled data. Cells are colored by their scMEP state (right). **b**, UMAP visualization of CD4$^+$ T cell states as in a colored by normalized (99.9th percentile) expression of the indicated proteins. **c**, Marker enrichment modeling was used to visualize enrichment (purple) or depletion (yellow) of metabolic regulator (left) expression and immune phenotype (right) across CD4$^+$ T cell states. **d**, Frequencies of state across individual samples. **e**, Statistical comparison of scMEP state frequencies. P-values were calculated using a two-sided, paired t-test between healthy and malignant colon sections from the same patient. Welch correction was applied to account for potentially differing variances. scMEP9: Estimate = -9.22, t-statistic = -2.87, CI -17.5 to -0.95, 5 degrees of freedom, BH FDR = 0.239. scMEP12: Estimate = -0.29, t-statistic = -2.81, CI -0.56 to -0.03, 5 degrees of freedom, BH FDR = 0.239. P-values not stated when P > 0.05. **f**, Comparison of metabolic and immunological marker expression on three selected CD4$^+$ T cell states as defined in a-d.
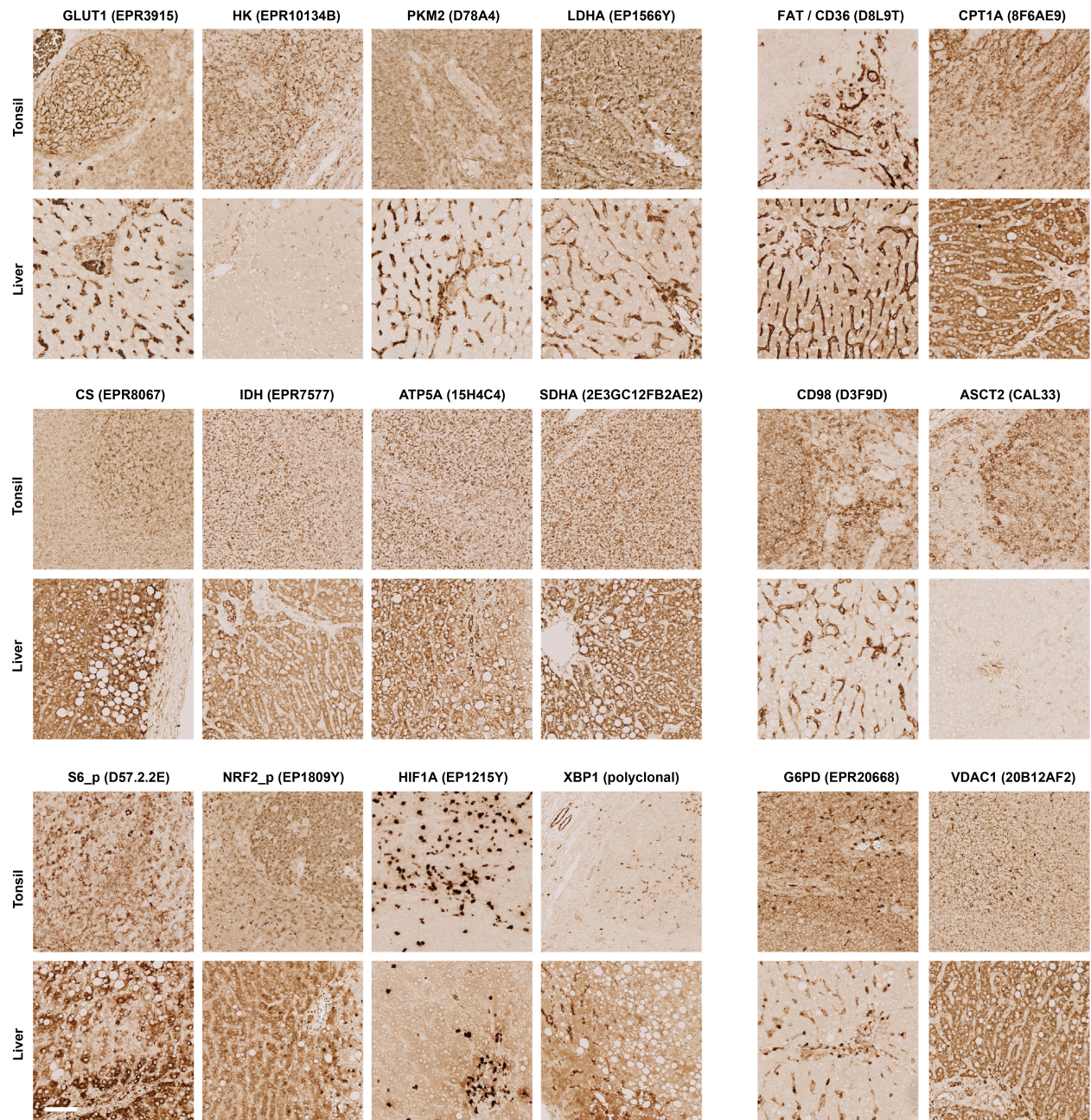
Supplementary Figure 11: Immunohistochemistry validation of metabolic antibodies. FFPE sections from healthy donor liver and tonsil tissues were stained by IHC with the indicated (metal-conjugated) antibodies for validation. Scale bar = 100 μm.
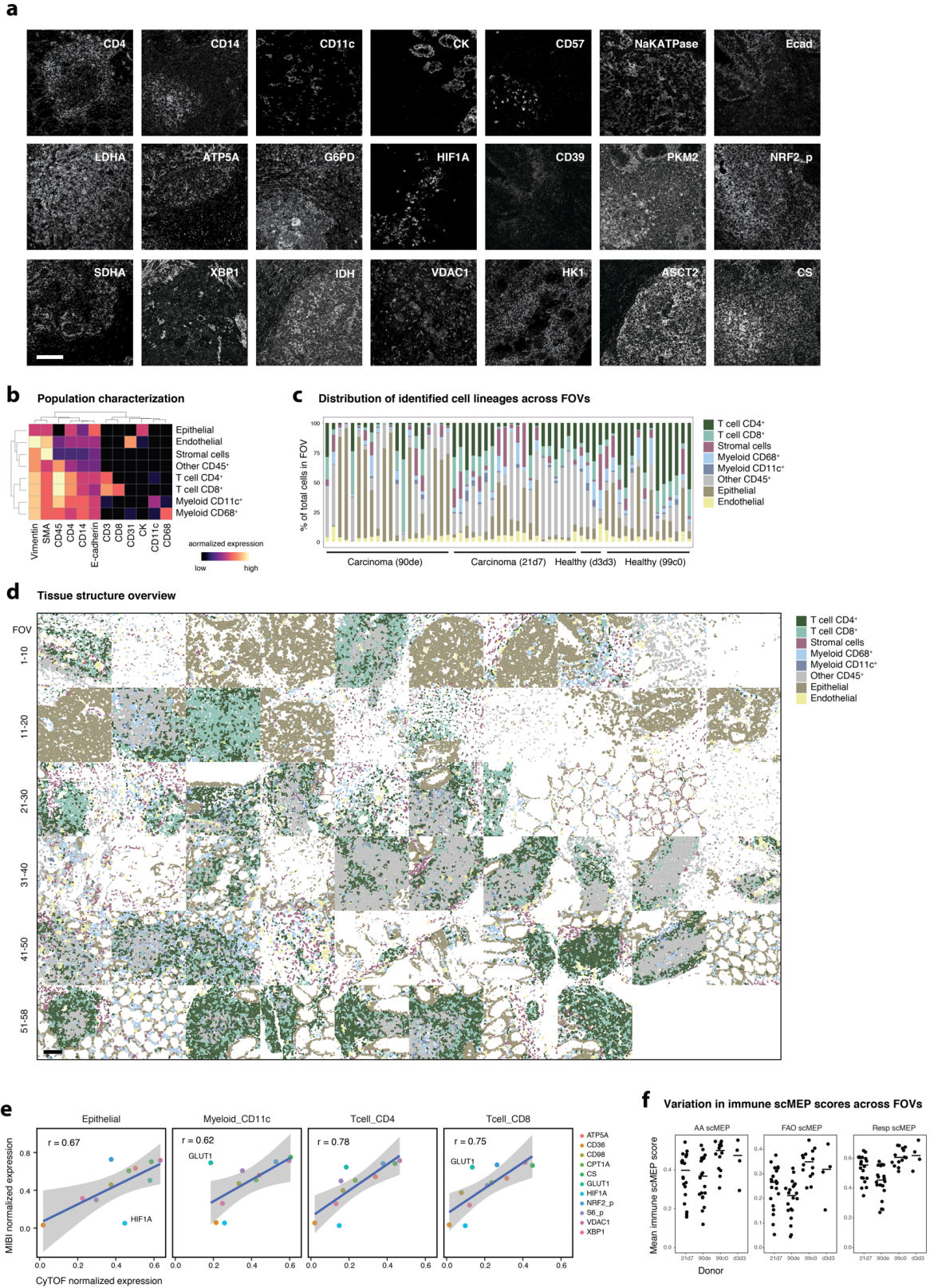
a

b Population characterization

c Distribution of identified cell lineages across FOVs

d Tissue structure overview

e

f Variation in immune scMEP scores across FOVs

Supplementary Figure 12: Imaging-based analysis of metabolic states in human colorectal carcinoma. a, Exemplary grayscale images showing staining of lineage and metabolic antibodies in human colorectal FFPE sections imaged by MIBI-TOF.

15

Scale bar = 100 μm. **b**, Single cells were segmented from all images and clustered into the main cell lineages using FlowSOM. Heatmap values represent scaled and normalized mean expression values of the indicated population. **c**, Composition of each field of view (FOV) based on clustering results as in b. **d**, Segmented and clustered cells can be visualized in their original location on the image. FOVs are numbered 1-58 from left to right and top to bottom. **e**, Linear regression of mean metabolic regulator expression on the indicated cell populations between CyTOF and MIBI-TOF data. r values and blue lines are results of linear regression analysis with black shading representing the 95% CI. **f**, Average scMEP scores for all CD45$^+$ cells within a FOV. AA = Amino acid. FAO = Fatty acid oxidation. Resp = respiration. Black lines indicate donor means.
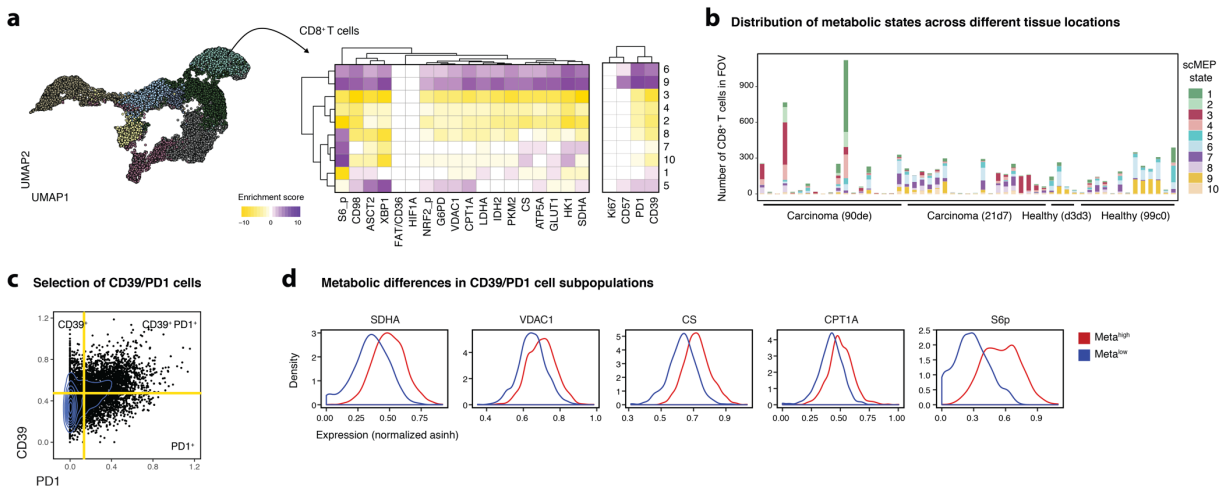
Supplementary Figure 13: Imaging-based analysis of metabolic CD8+ T cell subsets. a, UMAP dimensionality reduction overview of segmented MIBI-TOF data with cells colored by their immune cell lineage (left). CD8+ T cells were selected and clustered into ten scMEP states using only metabolic features as input dimensions (right). Heatmap indicates mean MEM enrichment scores across all scMEP states. **b,** Absolute numbers of scMEP states as defined in a across individual field of views (FOVs). **c,** CD39 and PD1 expression on CD8+ T cells across all FOVs. CD39/PD1 cells were defined using the indicated yellow lines. **d,** CD39/PD1 cells defined as in c were clustered into two subsets using FlowSOM and their metabolic regulome profile as input. Histograms display the marker expression levels of the two clusters, termed Meta^high (red) and Meta^low (blue).